



THE UNIVERSITY *of* EDINBURGH

Edinburgh Research Explorer

Direct observation of the ferrimagnetic coupling of A-site Cu and B-site Fe spins in charge-disproportionated $\text{CaCu}_3\text{Fe}_4\text{O}_{12}$

Citation for published version:

Mizumaki, M, Chen, WT, Saito, T, Yamada, I, Attfield, JP & Shimakawa, Y 2011, 'Direct observation of the ferrimagnetic coupling of A-site Cu and B-site Fe spins in charge-disproportionated $\text{CaCu}_3\text{Fe}_4\text{O}_{12}$ ', *Physical review B*, vol. 84, no. 9, 094418, pp. -. <https://doi.org/10.1103/PhysRevB.84.094418>

Digital Object Identifier (DOI):

[10.1103/PhysRevB.84.094418](https://doi.org/10.1103/PhysRevB.84.094418)

Link:

[Link to publication record in Edinburgh Research Explorer](#)

Document Version:

Publisher's PDF, also known as Version of record

Published In:

Physical review B

Publisher Rights Statement:

Copyright © 2011 The American Physical Society. This article may be downloaded for personal use only. Any other use requires prior permission of the author and the American Physical Society.

General rights

Copyright for the publications made accessible via the Edinburgh Research Explorer is retained by the author(s) and / or other copyright owners and it is a condition of accessing these publications that users recognise and abide by the legal requirements associated with these rights.

Take down policy

The University of Edinburgh has made every reasonable effort to ensure that Edinburgh Research Explorer content complies with UK legislation. If you believe that the public display of this file breaches copyright please contact openaccess@ed.ac.uk providing details, and we will remove access to the work immediately and investigate your claim.



Direct observation of the ferrimagnetic coupling of A-site Cu and B-site Fe spins in charge-disproportionated $\text{CaCu}_3\text{Fe}_4\text{O}_{12}$

M. Mizumaki,^{1,2} W. T. Chen,³ T. Saito,^{2,3} I. Yamada,^{3,*} J. Paul Attfield,⁴ and Y. Shimakawa^{2,3}¹*Japan Synchrotron Radiation Research Institute, SPring-8, 1-1-1 Kouto, Sayo-cho, Sayo-gun, Hyogo 679-5198, Japan*²*Core Research for Evolutional Science and Technology, Japan Science and Technology Agency,**5 Sanbancho, Chiyoda ku, Tokyo 102-0075, Japan*³*Institute for Chemical Research, Kyoto University, Gokasho, Uji, Kyoto 611-0011, Japan*⁴*Centre for Science at Extreme Conditions and School of Chemistry, University of Edinburgh, Mayfield Road, Edinburgh EH9 3JZ, Scotland, United Kingdom*

(Received 16 May 2011; published 15 September 2011)

The magnetic coupling between Fe and Cu moments in the charge-disproportionated $\text{CaCu}_3\text{Fe}_4\text{O}_{12}$ is studied by neutron powder diffraction, x-ray absorption, and magnetic circular dichroism measurements. The magnetic moments of the B-site Fe are coupled antiferromagnetically with those of the A'-site Cu, and the Fe^{3+} and Fe^{5+} spins at the B site align ferromagnetically. The orbital contribution of the magnetic moment for Fe is significant and appears to stabilize the ferrimagnetic structure of charge-disproportionated $\text{CaCu}_3\text{Fe}_4\text{O}_{12}$.

DOI: [10.1103/PhysRevB.84.094418](https://doi.org/10.1103/PhysRevB.84.094418)

PACS number(s): 75.47.Lx, 78.70.Dm, 75.25.-j

I. INTRODUCTION

A-site ordered perovskite oxides, $\text{A}'\text{A}_3\text{B}_4\text{O}_{12}$, contain transition-metal ions at both A' and B sites, in square planar and octahedral coordination by oxygen ions, respectively. When the A'- and B-site ions are magnetic species, A'-A' and A'-B magnetic interactions are observed in addition to the B-B interaction seen in many ABO_3 perovskite oxides.¹ For example, A' (Cu^{2+})-A' (Cu^{2+}) ferromagnetic interactions are observed in $\text{CaCu}_3\text{Sn}_4\text{O}_{12}$ and $\text{CaCu}_3\text{Ge}_4\text{O}_{12}$, whereas A' (Cu^{2+})-A' (Cu^{2+}) antiferromagnetic interactions are observed in $\text{CaCu}_3\text{Ti}_4\text{O}_{12}$.²⁻⁴ In $\text{CaCu}_3\text{Mn}_4\text{O}_{12}$, on the other hand, A'-site Cu^{2+} spins couple with B-site Mn^{4+} spins antiferromagnetically, leading to a ferrimagnetic state below the transition temperature at approximately room temperature.⁵ Even for $\text{LaCu}_3\text{Mn}_4\text{O}_{12}$ and $\text{BiCu}_3\text{Mn}_4\text{O}_{12}$, A'-site Cu^{2+} spins antiferromagnetically couple with magnetic spins of the mixed valence $\text{Mn}^{3.75+}$.⁶ Thus, A-site ordered perovskite oxides with magnetic species at both A' and B sites provide opportunities to study a wide variety of magnetic ground states in oxides.

$\text{CaCu}_3\text{Fe}_4\text{O}_{12}$ (CCFO) is a newly synthesized compound with the magnetic Cu and Fe ions at A' and B sites, respectively. Although $\text{CaCu}_3\text{Fe}_4\text{O}_{12}$ is paramagnetic at room temperature, it shows charge disproportionation (CD) of B-site Fe ions, that is, $2\text{Fe}^{4+} \rightarrow \text{Fe}^{3+} + \text{Fe}^{5+}$, at $T_{\text{CD}} = 210$ K, and a large magnetization was observed below the CD transition temperature.⁷ The observed magnetic properties of CCFO are quite different from those of the simple perovskite CaFeO_3 , in which the charge-disproportionated Fe spins produced a complicated helicoidal antiferromagnetic spin structure.⁷ The magnetic structure of CCFO was tentatively assumed to be ferrimagnetic by analogy with that of $\text{CaCu}_3\text{Mn}_4\text{O}_{12}$; however, the magnetic coupling between the Cu and Fe ions in CCFO has not yet been clarified in detail.

In this paper, we report the magnetic structure and the magnetic coupling of Cu and Fe spins in CCFO from the analysis of neutron powder diffraction (NPD), the x-ray-absorption spectroscopy (XAS), and magnetic circular dichroism (MCD) measurements. We also discuss the contribution of the orbital

magnetic moment in stabilizing the ferrimagnetic structure of charge-disproportionated CCFO.

II. EXPERIMENTAL PROCEDURES

A ~ 300 mg powder sample of CCFO was synthesized under a high-pressure and high-temperature condition, and the details of the sample synthesis were described in Ref. 7. The obtained sample was confirmed to be single phase by x-ray diffraction.

Time-of-flight NPD data from a polycrystalline sample were collected on the PEARL instrument at the ISIS facility in the United Kingdom. The diffraction data at 300 and 120 K, which are respectively above and below T_{CD} , were collected by a detector bank covering the scattering angle range $83 \leq 2\theta \leq 97^\circ$ giving a d-spacing range of $\sim 0.5\text{--}4.1$ Å. The crystal and magnetic structures were analyzed from the diffraction data with the Rietveld method using the General Structure Analysis System software package.^{8,9}

The XAS and MCD for Cu $L_{3,2}$, Fe $L_{3,2}$, and O K edges for the disproportionated CCFO were measured at 9 K by a total electron yield method at BL25SU of SPring-8 in Japan. The energy resolution $E/\Delta E$ at the Cu $L_{3,2}$ and Fe $L_{3,2}$ edges was greater than 5000. The incident photon energy was calibrated by measuring the energies of the Ti $L_{3,2}$ edges of TiO_2 and the Ni $L_{3,2}$ edges of NiO. A powder sample was pasted uniformly on a sample holder by using carbon tape. The spectra were obtained using parallel (I_+) and antiparallel (I_-) photon spins along the magnetization direction of the sample, to which a static magnetic field of 1.9 T was applied. The MCD intensity was defined by the difference between the two absorption spectra ($I_{\text{MCD}} = I_- - I_+$).

III. RESULTS AND DISCUSSION

The neutron-diffraction peaks of CCFO observed at 300 K were indexed with the $Im\bar{3}$ (No. 204) space group with the lattice parameter $a = 7.29667(6)$ Å, and the atom positions were refined to be Ca $2a$ (0, 0, 0), Cu $6b$ (0, 1/2, 1/2), Fe $8c$ (1/4, 1/4, 1/4), and O $24g$ [0.3070(1), 0.1760(2), 0]. A satisfactory fit with the residuals $R_{\text{wp}} = 4.10\%$ and $\chi^2 = 2.76$ was achieved,

and the refined structural parameters were essentially the same as those reported previously.⁷ Thus, the result confirmed that the material was crystallized with the A-site ordered perovskite with the charge composition of $\text{CaCu}^{2+}_3\text{Fe}^{4+}_4\text{O}_{12}$.

The diffraction data at 120 K ($< T_{\text{CD}}$) contain additional peaks that evidence the charge-disproportionated state of CCFO with the $Pn-3$ (No. 201) space group with the cubic lattice parameter $a = 7.26627(9)$ Å. The atom positions Ca 2a (1/2, 1/2, 1/2), Cu 6d (1/2, 0, 0), Fe1 4b (1/4, 1/4, 1/4), Fe2 4c (3/4, 3/4, 3/4), and O 24h [0.5036(9), 0.1939(2), 0.3223(2)] obtained from the refinement produced two distinct Fe-O distances, 1.959(7) and 1.910(7) Å. The bond valence sum calculations gave Fe ionic states of +3.42 and +4.13 for Fe1(Fe^{3+}) and Fe2(Fe^{5+}), respectively, although the apparent charge difference is less than expected for the ideal charge states, as is observed in most charge-ordered oxides.¹⁰

Magnetic contributions to some of the neutron-diffraction peaks are clearly seen at 120 K, as shown in Fig. 1. The magnetic diffraction peaks coincide with the nuclear ones, showing that no magnetic superstructure is present. Rietveld analysis of the magnetic structure achieved the fitting residuals $R_{\text{wp}} = 5.01\%$ and $\chi^2 = 1.82$. The refined (z -axis) magnetic moments at the Fe1(Fe^{3+}), Fe2(Fe^{5+}), and Cu sites were 3.3(2), 1.9(2), and $-0.6(1)$ μ_B , respectively, showing that the refined moment at the square-planar-coordinated 6d Cu

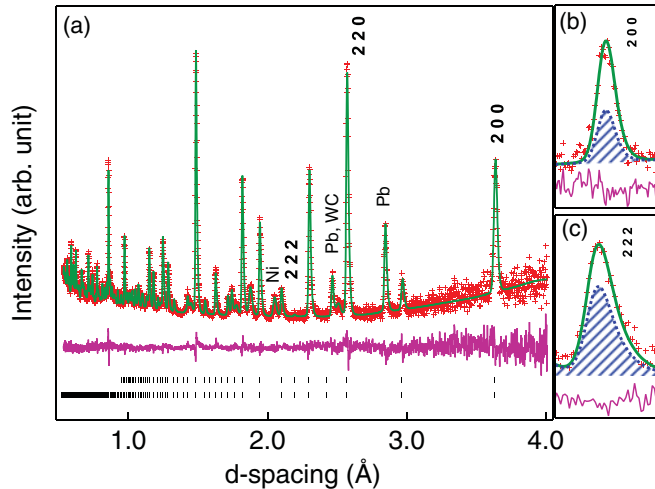


FIG. 1. (Color) Observed (+), calculated (solid line), and difference (bottom) NPD Rietveld profiles for $\text{CaCu}_3\text{Fe}_4\text{O}_{12}$ at 120 K, where the bottom and top index markers correspond to the reflections of crystal and magnetic structures, respectively. The representative Bragg peaks of pressure calibrant Pb, instrumental tungsten carbide (WC) and Ni, and the magnetic reflections 200, 220, and 222 of $\text{CaCu}_3\text{Fe}_4\text{O}_{12}$ are also labeled in the figure. The representative magnetic peaks 200 and 222 are respectively shown in (b) and (c), where the break line with shaded area indicates the nuclear reflection and the solid line corresponds to the reflection with magnetic contribution. NPD data at 120 K were obtained with a Paris-Edinburgh cell, with which a high-pressure environment can be applied. A pressure transmission medium of a methanol/ethanol mixture and a pressure calibrant Pb pellet were sealed into the gasket with the sample. The data were collected without cell pressurization for 8 h. The results of the high-pressure study of CCFO will be reported elsewhere.

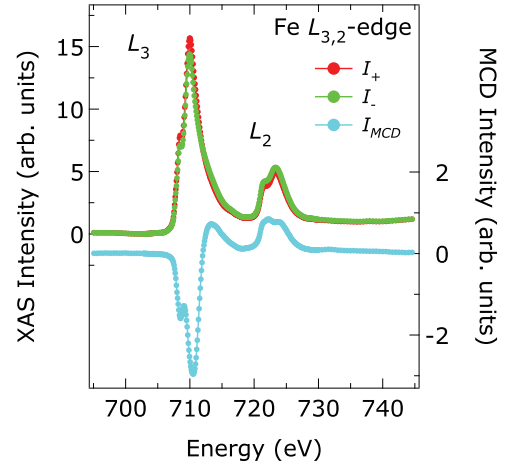


FIG. 2. (Color) XAS and MCD spectra at Fe $L_{3,2}$ edges for $\text{CaCu}_3\text{Fe}_4\text{O}_{12}$ at $T = 9$ K. Red (I_+) and green (I_-) circles show the XAS spectra measured with external field 1.9 T applied parallel and antiparallel to the light propagation axis. The bottom line represents the MCD intensity I_{MCD} . The arbitrary unit of intensity in the XAS spectrum was set to unity at 737 eV.

site is antiparallel to the B-site Fe^{3+} and Fe^{5+} spins. The three moments are reduced to 60–66% of their ideal values, showing that the metal-oxygen bonds are strongly covalent. Spin canting models with M_x and M_y components at the Fe sites were also examined, but no convincing result was obtained. The total moment can thus be calculated to be ~ 8.6 μ_B , which is in a good agreement with the previously reported saturated magnetization moment of ~ 8.3 μ_B at 100 K.⁷

The result is consistent with a ferrimagnetic structure model, which we assumed tentatively in our previous paper.⁷ Because the magnetic ordering occurred at the CD transition temperature as confirmed by Mössbauer and magnetic measurements, the ferrimagnetic structure is stabilized with the CD electronic state.

Figure 2 shows the I_+ and I_- XAS spectra at the Fe $L_{3,2}$ edges. Although the two Fe sites, i.e., charge-disproportionated Fe^{3+} and Fe^{5+} , were distinguished in the neutron structure analysis, the corresponding two components in the spectra were not evident. Because the 3d levels in Fe are very close to the 2p levels in oxygen so that the electronic structures of Fe^{3+} and Fe^{5+} may be considered as $3d^5$ and $3d^5\bar{L}^2$ (where \bar{L} is a ligand hole), respectively, the XAS spectra for Fe^{3+} and Fe^{5+} should be quite similar. Thus, the observed spectra represent the average electronic structure for Fe^{3+} and Fe^{5+} . The spectral shape is very similar to that observed in $\text{SrFe}_{1-x}\text{Mn}_x\text{O}_3$ ($0 < x < 1$) with charge-disproportionated states.^{11–14} The MCD intensities at the Fe L_3 edge (~ 710 eV) are negative, whereas those at the Fe L_2 edge (~ 723 eV) are positive. The I_+ and I_- XAS spectra at the $L_{3,2}$ edges are also shown in Fig. 3. This spectral shape is similar to that of $\text{BiCu}_3\text{Mn}_4\text{O}_{12}$ containing typical divalent Cu ions.¹⁵ The MCD intensities at the Cu L_3 edge (~ 931.5 eV) are positive, while those at the Cu L_2 edge (~ 951.3 eV) are negative.

The result that the signs of the MCD intensities at the L_3 and L_2 edges between Fe and Cu are opposite indicates that the magnetic coupling between the Fe and Cu spins is antiferromagnetic. The MCD results are consistent with the

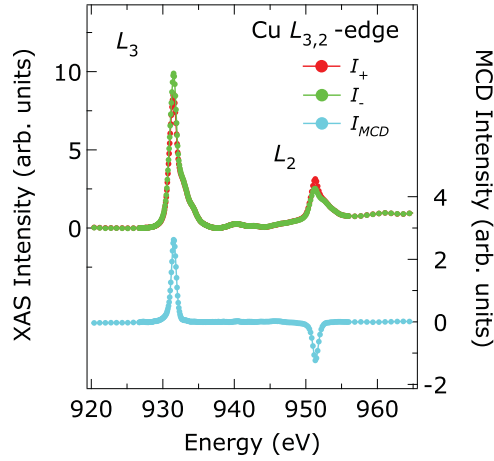


FIG. 3. (Color) XAS and MCD spectra at Cu $L_{3,2}$ edges for $\text{CaCu}_3\text{Fe}_4\text{O}_{12}$ at $T = 9$ K. Red (I_+) and green (I_-) circles show the XAS spectra measured with external field 1.9 T applied parallel and antiparallel to the light propagation axis. The bottom line represents the MCD intensity I_{MCD} . The arbitrary unit of intensity in the XAS spectrum was set to unity at 965 eV.

magnetic structure obtained from neutron analysis, in which the magnetic moments of Fe and Cu align antiferromagnetically. We can thus conclude that the charge-disproportionated CCFO is a ferrimagnet as previously assumed.⁷ All the results of the NPD and MCD experiments indicate that the antiferromagnetic coupling between the A'-site Cu and B-site Fe spins is dominant in charge-disproportionated CCFO and that the B-site Fe^{3+} and Fe^{5+} spins align ferromagnetically as do the A'-site Cu spins. This is in sharp contrast to the magnetic interaction seen in CaFeO_3 , where B-site antiferromagnetic interaction is dominant, producing the helicoidal antiferromagnetic spin structure in the charge-disproportionated state.

Figure 4 shows the XAS spectrum $[(I_- + I_+)/2]$ at the O K edge, which originates from an excitation of electrons from the O $1s$ state to the unoccupied O $2p$ states in the conduction band. Since the empty O $2p$ states hybridize with the $3d$ and $4sp$ states of cations in oxides, the observed O-XAS spectrum reflects the features of the electronic structures of the constituent transition-metal ions.¹⁶ The spectrum from 527 to 530 eV mainly represents the nature of the Fe $3d$ bands, while that at approximately 532 eV shows the nature of the Cu $3d$ bands (the upper Hubbard band). The absorption spectrum at approximately 540–545 eV reflects the characters of the Cu $4sp$ and Fe $4sp$ bands.^{2,14,16} In the MCD spectrum, also shown in Fig. 4, it is notable that negative signals are clearly observed around the Fe $3d$ region but are not so evident for the Cu $3d$ region. As seen in $\text{La}_{1-x}\text{Sr}_x\text{MnO}_{3+\delta}$,¹⁷ the negative MCD signal at the O K edge with intensity of a few percent of the XAS suggests the contribution of a direct transfer from the $3d$ orbital magnetic moment of a transition metal to the O $2p$ states. Thus, the result of the O K -edge MCD indicates that Fe $3d$ orbital magnetic moments contributed to the magnetic properties of the ferrimagnetic CCFO.

We quantitatively analyze the orbital magnetic moment of Fe and Cu ions in CCFO by using the magneto-optical

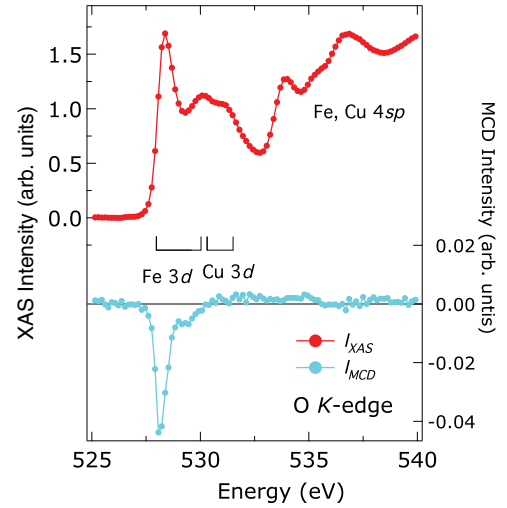


FIG. 4. (Color) XAS and MCD spectra at O K edges for $\text{CaCu}_3\text{Fe}_4\text{O}_{12}$ at $T = 9$ K. Red circles show the XAS spectrum $I_{\text{XAS}} = [(I_- + I_+)/2]$ measured with external field 1.9 T applied parallel and antiparallel to the light propagation axis. The bottom line represents the MCD intensity I_{MCD} . The arbitrary unit of intensity in the XAS spectrum was set to unity at 552 eV.

sum rules.^{18,19} The total magnetic moment (M_{total}) consists of orbital (M_{orb}) and spin (M_{spin}) parts, and they are expressed as

$$M_{\text{orb}} = -\frac{4n_h}{3} \left(\frac{I_{L_3} + I_{L_2}}{W_{L_3} + W_{L_2}} \right), \quad (1)$$

$$M_{\text{spin}} = -n_h \left(\frac{I_{L_3} - 2I_{L_2}}{W_{L_3} + W_{L_2}} \right), \quad (2)$$

where I and W represent the spectral weights of the MCD and XAS intensities, respectively, and n_h is the number of holes in the $3d$ state. The boundaries between the L_3 and L_2 edges of the Fe and Cu spectra are set to 719.3 and 946.5 eV, respectively. Because the sample is a polycrystal and the Fe and Cu ions in CCFO are located at the high-symmetry O_h and D_{4h} sites, respectively, the magnetic dipole matrix operator is zero and thus the M_{spin} is simplified as in Eq. (2). From an *ab initio* band calculation with the local spin-density approximation, n_h for Fe- $3d$ and Cu- $3d$ were estimated to be 3.75 and 0.7, respectively.¹¹ With these values, we can obtain $M_{\text{spin}} = 3.49 \pm 0.01 \mu_B$, $M_{\text{orb}} = -0.07 \pm 0.01 \mu_B$, and thus $M_{\text{total}} = 3.41 \pm 0.02 \mu_B$ per Fe ion and $M_{\text{spin}} = -0.52 \pm 0.01 \mu_B$, $M_{\text{orb}} = -0.02 \pm 0.01 \mu_B$, and $M_{\text{total}} = -0.54 \pm 0.02 \mu_B$ per Cu ion. The orbital part of the magnetic moment for Fe is significant, consistent with the observation of the O K -edge MCD spectrum.

In a simple perovskite, SrFeO_3 , with high-valence Fe^{4+} ions, no orbital magnetic contribution of Fe $3d$ was observed in the XAS-MCD spectra.¹² Considering that SrFeO_3 shows a complicated helical magnetic structure, the orbital magnetic moments of Fe ions in the present CCFO appear to play an important role in stabilizing the ferrimagnetic structure in the CD state.

IV. CONCLUSION

We have investigated the magnetic structure of the recently discovered A-site ordered perovskite $\text{CaCu}_3\text{Fe}_4\text{O}_{12}$ and confirmed the magnetic coupling between A'-site Cu and B-site Fe spins. Analysis of the NPD data taken at 120 K, where the material showed charge disproportionation, reveals a ferrimagnetic spin structure with refined magnetic moments of $-0.6(1) \mu_B$ for the A-site Cu and $3.3(2)$ and $1.9(2) \mu_B$ for the B-site Fe^{3+} and Fe^{5+} , respectively. From the XAS measurements around the $\text{Fe-}L_{3,2}$ and $\text{Cu-}L_{3,2}$ edges, MCD signals were clearly observed, and the sign of signals for Fe was opposite to that for Cu, also confirming the antiferromagnetic coupling between the Fe and Cu spins. Applying the sum rules to the spectra, the orbital and spin magnetic moments were obtained to be $M_{\text{spin}} = 3.49 \mu_B$ and $M_{\text{orb}} = -0.07 \mu_B$ for Fe and $M_{\text{spin}} = -0.52 \mu_B$ and $M_{\text{orb}} = -0.02 \mu_B$ for Cu. The orbital magnetic contribution to the magnetic moment of Fe is significant and may play an important role in stabilizing the A'-B antiferromagnetic interaction in the charge-disproportionated ferrimagnet $\text{CaCu}_3\text{Fe}_4\text{O}_{12}$.

ACKNOWLEDGMENTS

We are grateful to Ms. A. Sinclair (The University of Edinburgh) and Dr. M. Tucker (ISIS), for their help in the neutron powder diffraction measurements at the PEARL diffractometer. We also thank Professor M. Takano (Kyoto University) and Dr. S. Kimura (JASRI) for their support during the work. M. Mizumaki thanks Professor T. Mizokawa (Tokyo University) and Dr. J. Matusno (RIKEN) for their useful discussions. The neutron-diffraction experiments were done under the Strategic Japanese-UK Cooperative Program by Japan Science and Technology Agency (JST) and Engineering and Physical Sciences Research Council (EPSRC). The XAS-MCD measurements at BL25SU (Proposal No. 2008A1001) in SPring-8 were performed with the approval of the Japan Synchrotron Radiation Research Institute. This work was partly supported by a Grant-in-Aid for Scientific Research (Grant No. 19GS0207) and by the Global Center of Excellence (COE) Program Integrated Materials Science (No. B-09) from the Ministry of Education, Science, and Technology of Japan and by the JST CREST. Support was also provided by EPSRC and the Leverhulme Trust, United Kingdom.

*Present address: Department of Chemistry, Graduate School of Science and Engineering, Ehime University, 2-5 Bunkyo-cho, Matsuyama, Ehime 790-8577, Japan.

¹Y. Shimakawa, *Inorg. Chem.* **47**, 8562 (2008).

²M. Mizumaki, T. Saito, H. Shiraki, and Y. Shimakawa, *Inorg. Chem.* **48**, 3499 (2009).

³H. Shiraki, T. Saito, T. Yamada, M. Tsujimoto, M. Azuma, H. Kurata, S. Isoda, M. Takano, and Y. Shimakawa, *Phys. Rev. B* **76**, 140403 (2007).

⁴Y. Shimakawa, H. Shiraki, and T. Saito, *J. Phys. Soc. Jpn.* **77**, 113702 (2008).

⁵Z. Zeng, M. Greenblatt, M. A. Subramanian, and M. Croft, *Phys. Rev. Lett.* **82**, 3164 (1999).

⁶J. A. Alonso, J. Sánchez-Benítez, A. De Andrés, M. G. Martínez-Lope, M. T. Casais, and J. L. Martínez, *Appl. Phys. Lett.* **83**, 2623 (2003).

⁷I. Yamada, K. Takata, N. Hayashi, S. Shinohara, M. Azuma, S. Mori, S. Muranaka, Y. Shimakawa, and M. Takano, *Angew. Chem. Int. Ed.* **47**, 7032 (2008).

⁸A. C. Larson and R. B. Von Dreele, Los Alamos National Laboratory Report LAUR 86-748, 2004.

⁹B. H. Toby, *J. Appl. Crystallogr.* **34**, 210 (2001).

¹⁰J. P. Attfield, *Solid State Sci.* **8**, 861 (2006).

¹¹X. Hao, Y. Xu, F. Gao, D. Zhou, and J. Meng, *Phys. Rev. B* **79**, 113101 (2009).

¹²J. Okamoto *et al.*, *Phys. Rev. B* **71**, 104401 (2005).

¹³M. Abbatte, G. Zampieri, J. Okamoto, A. Fujimori, S. Kawasaki, and M. Takano, *Phys. Rev. B* **65**, 165120 (2002).

¹⁴T. Koide, T. Shidara, H. Miyauchi, N. Nakjima, H. Fukutani, A. Fujimori, S. Kawasaki, M. Takano, and Y. Takeda, *J. Magn. Soc. Jpn.* **23**, 341 (1999).

¹⁵T. Saito, W. T. Chen, M. Mizumaki, J. P. Attfield, and Y. Shimakawa, *Phys. Rev. B* **82**, 024426 (2010).

¹⁶M. Abatte *et al.*, *J. Electron Spectrosc. Relat. Phenom.* **62**, 185 (1993).

¹⁷T. Koide, H. Miyauchi, J. Okamoto, T. Shidara, T. Sekine, T. Saitoh, A. Fujimori, H. Fukutani, M. Takano, and Y. Takeda, *Phys. Rev. Lett.* **87**, 246404 (2001).

¹⁸B. T. Thole, P. Carra, F. Sette, and G. van der Laan, *Phys. Rev. Lett.* **68**, 1943 (1992).

¹⁹P. Carra, B. T. Thole, M. Altarelli, and X. Wang, *Phys. Rev. Lett.* **70**, 694 (1993).